

Supporting Information:

Eutectoid nano-precipitations inducing remarkably enhanced thermoelectric performance in $(\text{Sn}_{1-x}\text{Cd}_x\text{Te})_{1-y}(\text{Cu}_2\text{Te})_y$

Xia Qi,^{†ab} Yi Huang,^{†b} Di Wu,^{*a} Binbin Jiang,^b Bin Zhu,^b Xiao Xu,^b Jianghe Feng,^b Baohai Jia,^b Zhong Shu,^b Jiaqing He^{*b}

^a Key Laboratory for Macromolecular Science of Shaanxi Province, School of Materials Science and Engineering, Shaanxi Normal University, Xi'an 710119, China

^b Department of Physics, Southern University of Science and Technology, Shenzhen 518055, China

[†] These authors contributed equally to this work.

* Emails: wud@snnu.edu.cn; hejq@sustc.edu.cn

Sample Synthesis

In order to synthesize sample of nominal composition $\text{Sn}_{1-x}\text{Cd}_x\text{Te}$ ($x=0, 0.01, 0.02, 0.03, 0.04, 0.05$ and 0.06), $(\text{Sn}_{0.95}\text{Cd}_{0.05}\text{Te})_{1-y}(\text{Cu}_2\text{Te})_y$ ($y=0.01, 0.03, 0.05, 0.07$ and 0.09) and $\text{Sn}_{0.8835}\text{Cd}_{0.0465}\text{Cu}_{0.14}\text{Te}_{1-z}\text{I}_z$ ($z=0.0025, 0.005, 0.01, 0.015, 0.02$ and 0.03), stoichiometric mixtures of high-purity raw materials Sn shots (99.999% Aladdin), Te ingots (99.999% Aladdin), Cd shots (99.99% Aladdin), SnI_2 shots (99.99% Aladdin) and Cu power (99.99% Aladdin) were evacuated and sealed in a quartz tube ($< 10^{-4}$ Pa), heated to 400 °C in 4 h and maintained at this temperature for 4 h and then slowly heated 1000 °C in 10 hours and kept at that temperature for another 12 hours. The furnace shuts down and cools to room temperature. The obtained ingots were then hand milled into powders and finally sintered by spark plasma sintering system (SPS-211Lx, Japan) at 550 °C under 50 MPa for 5 minutes. Obtained pellets (all of density $>96\%$) were then cut into rectangular pieces $\sim 12 \times 2 \times 2$ mm for electrical transport measurements, while coins of $\Phi \sim 10$ mm and thickness ~ 1.5 mm were used for thermal diffusivity measurements.

X-Ray Diffraction and Electron Microscopy

The phase structure of samples was analyzed by X-ray diffraction (XRD) (Rigaku, Tokyo, Japan) at a scanning rate of 4° min^{-1} .

Transmission electron microscopy (TEM) was carried out using Thermo Fisher Talos F200X microscope operated at 200 kV.

Thermoelectric Properties Characterizations

The electrical resistivity and Seebeck coefficient were simultaneously measured from 323 to 823 K under helium atmosphere using a commercial ZEM-3 (Ulvac Riko, Japan) system. The uncertainties of the electrical resistivity and Seebeck coefficient measurements are both estimated to be about 5%. Thermal conductivity was calculated by $\kappa = D C_p \rho$. The thermal diffusivity D was measured in a state-of-art LFA 457 (Netzsch, Germany). For the specific heat C_p , we took the theoretical Dulong-Petit limit $3R/M$, where M is the average atomic mass per mol. Mas density was measured using the

Archimedes method, Table S1. The uncertainty of thermal conductivity is about 8%. Combining the uncertainties of all the measurements, the uncertainty of calculated ZT is less than 15%.

The total thermal conductivity (κ_{tot}) is composed of two contributions: the electron thermal conductivity (κ_{ele}) and the lattice thermal conductivity (κ_{lat}). The electron thermal conductivity κ_{ele} is proportional to the electrical conductivity σ through the Wiedemann-Franz¹ :

$$\kappa_{ele} = L \sigma T \quad (1)$$

where the Lorenz constant L can be estimated from a measured Seebeck coefficient based on a simplified model².

$$L = 1.5 + \text{EXP}(-S / 116) \quad (2)$$

The lattice thermal conductivity (k_{lat}) can be calculated by equal (3):

$$k_{lat} = k_{tot} - k_{ele} \quad (3)$$

Hall Measurements

Hall coefficient (R_H) was measured by the Van der Pauw method using a commercial Hall measurement system (Lake Shore 8400 Series, Model 8404, USA) from 323 K to 773 K. Then Hall carrier concentration (n_H) was estimated by $n_H = 1/eR_H$, and Hall carrier mobility (μ_H) was calculated by $\mu_H = R_H \sigma$.

Table S1. Mass densities $\rho(\text{g/cm}^3)$ of all samples investigated in this study.

Compositions	$\rho(\text{g/cm}^3)$	Compositions	$\rho(\text{g/cm}^3)$
SnTe	6.4732	(Sn _{0.95} Cd _{0.05} Te) _{0.95} (Cu ₂ Te) _{0.05}	6.4851
Sn _{0.99} Cd _{0.01} Te	6.4561	(Sn _{0.95} Cd _{0.05} Te) _{0.93} (Cu ₂ Te) _{0.07}	6.4885
Sn _{0.98} Cd _{0.02} Te	6.4575	(Sn _{0.95} Cd _{0.05} Te) _{0.91} (Cu ₂ Te) _{0.09}	6.484
Sn _{0.97} Cd _{0.03} Te	6.4369	(Sn _{0.95} Cd _{0.05} Te) _{0.93} (Cu ₂ Te) _{0.07-0.0025I}	6.49
Sn _{0.96} Cd _{0.04} Te	6.4442	(Sn _{0.95} Cd _{0.05} Te) _{0.93} (Cu ₂ Te) _{0.07-0.005I}	6.487
Sn _{0.95} Cd _{0.05} Te	6.4569	(Sn _{0.95} Cd _{0.05} Te) _{0.93} (Cu ₂ Te) _{0.07-0.01I}	6.4864
Sn _{0.94} Cd _{0.06} Te	6.4425	(Sn _{0.95} Cd _{0.05} Te) _{0.93} (Cu ₂ Te) _{0.07-0.015I}	6.4855
(Sn _{0.95} Cd _{0.05} Te) _{0.99} (Cu ₂ Te) _{0.01}	6.4654	(Sn _{0.95} Cd _{0.05} Te) _{0.93} (Cu ₂ Te) _{0.07-0.02I}	6.4868
(Sn _{0.95} Cd _{0.05} Te) _{0.97} (Cu ₂ Te) _{0.03}	6.4744	(Sn _{0.95} Cd _{0.05} Te) _{0.93} (Cu ₂ Te) _{0.07-0.03I}	6.4839

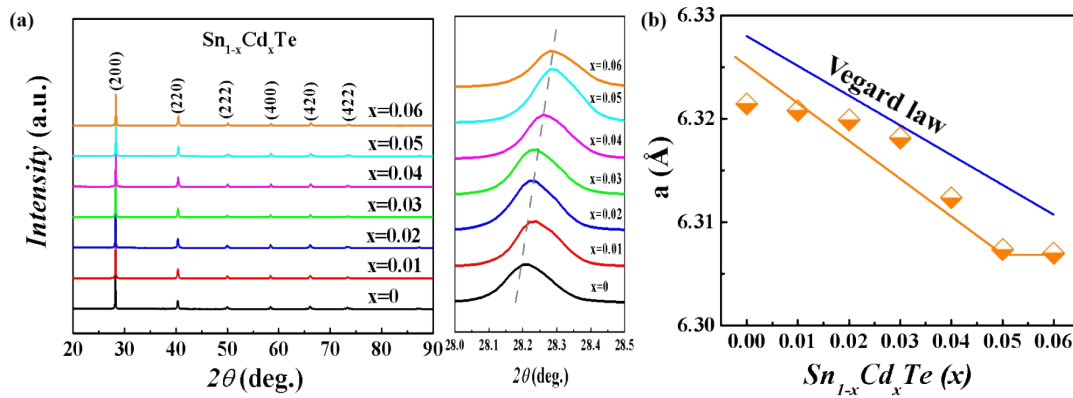


Fig.S1. (a) Powder X-ray diffraction (XRD) pattern and enlarged view of [200] Bragg peaks for the

Sn_{1-x}Cd_xTe samples ($x=0, 0.01, 0.02, 0.03, 0.04, 0.05$ and 0.06); (b) lattice parameter as a function of Cd content x .

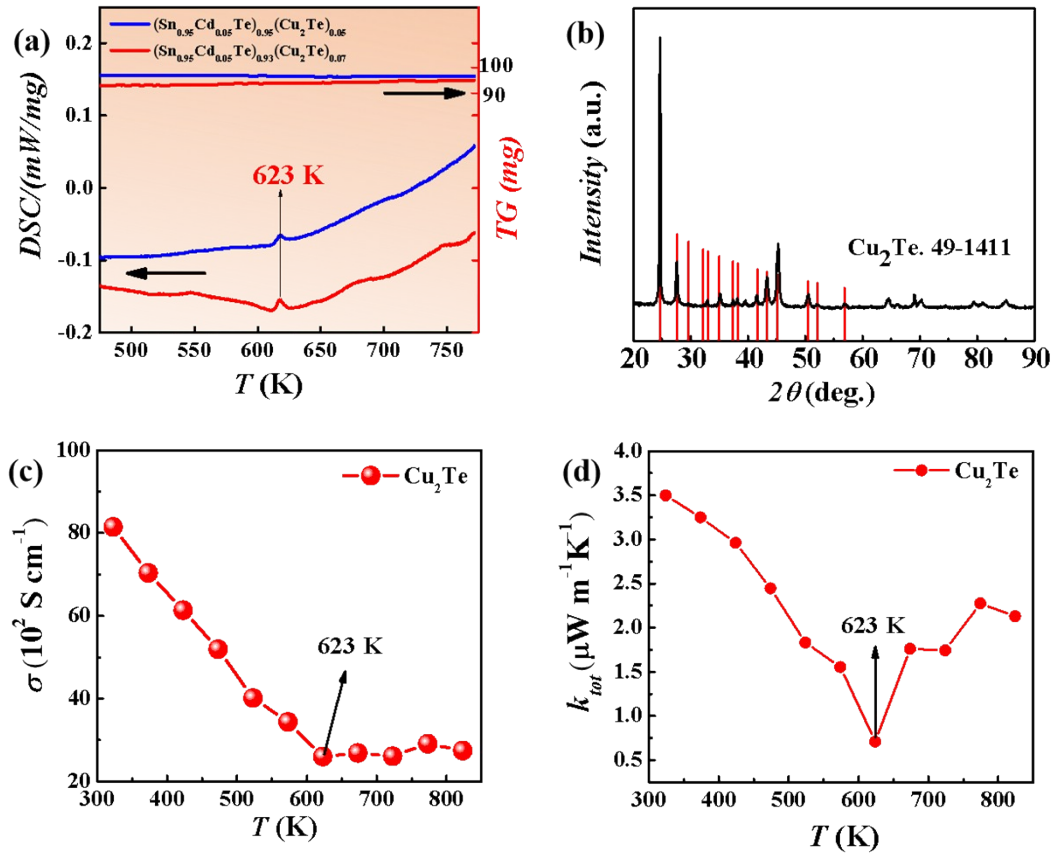


Fig.S2. The evidence of Cu₂Te secondary phase induced phase transition at ~ 623 K. (a) Differential scanning calorimetry (DSC) for Sn_{0.95}Cd_{0.05}Te and (Sn_{0.95}Cd_{0.05}Te)_{0.93}(Cu₂Te)_{0.07} samples. (b) XRD pattern; (c) electrical conductivity σ ; (d) thermal conductivity k_{tot} for Cu₂Te, suggesting the same kinks at 623 K.

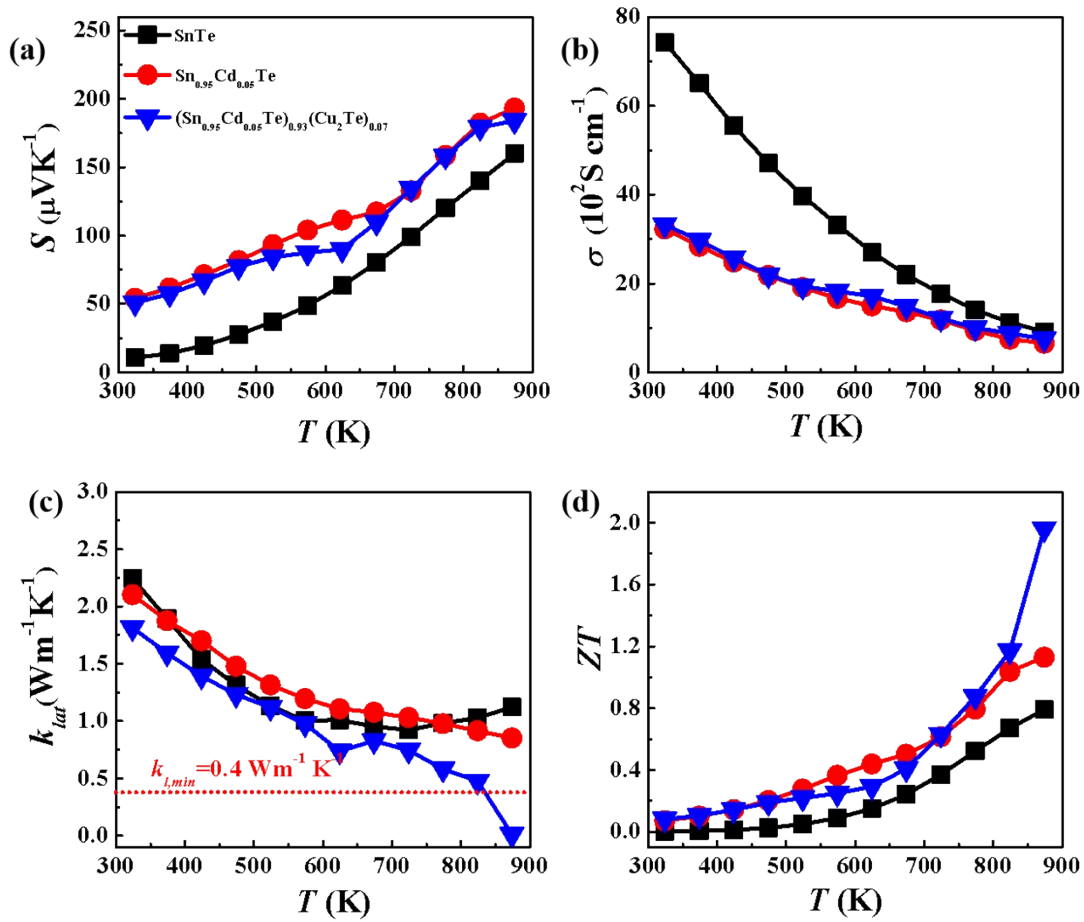


Fig. S3. (a) Seebeck coefficient S ; (b) electric conductivity σ ; (c) lattice thermal conductivity κ_{lat} ; (d) figure of merit ZT for SnTe; $\text{Sn}_{0.95}\text{Cd}_{0.05}\text{Te}$; $(\text{Sn}_{0.95}\text{Cd}_{0.05}\text{Te})_{0.95}(\text{Cu}_2\text{Te})_{0.05}$ samples. The extremely low lattice thermal conductivity over 823 K could probably come from the collapse of Cu_2Te secondary phase.

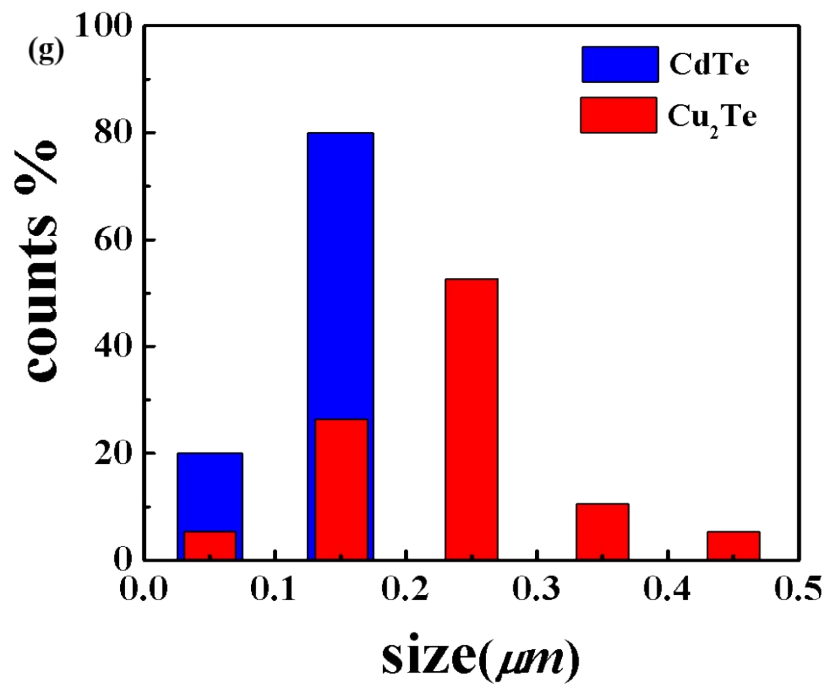
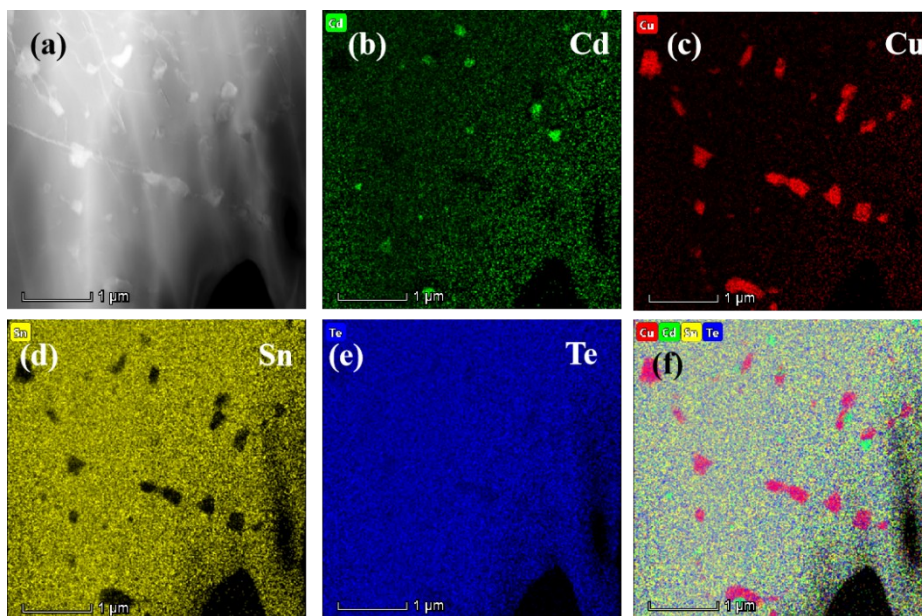


Fig.S4. (a) the HAADF-STEM image of $(\text{Sn}_{0.95}\text{Cd}_{0.05}\text{Te})_{0.93}(\text{Cu}_2\text{Te})_{0.07}$ sample and the corresponding EDS mapping (b-f), in which (f) is the mixed result; (g) the histograms of precipitate size for CdTe(blue) and Cu₂Te (red) in (f), respectively.

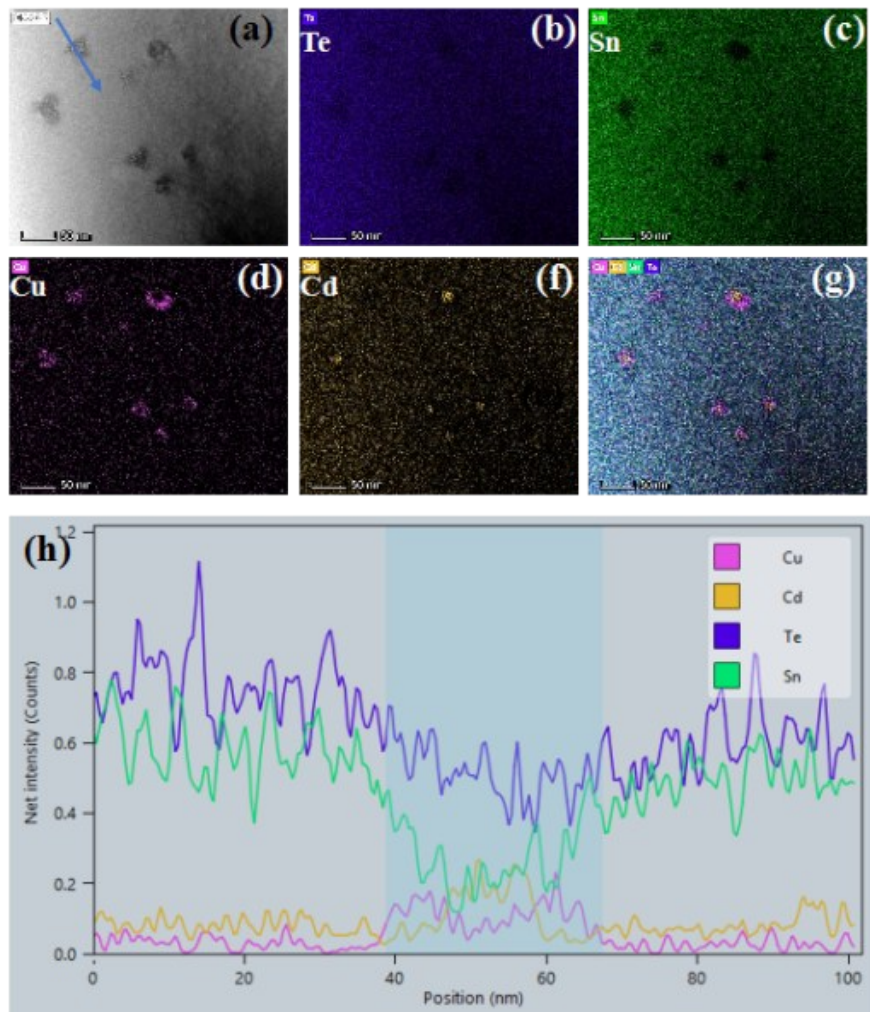


Fig.S5. (a) STEM-HAADF image of $(\text{Sn}_{0.95}\text{Cd}_{0.05}\text{Te})_{0.93}(\text{Cu}_2\text{Te})_{0.07}$ sample; (b-g) the EDS mapping of (a), in which (g) is the composite result; (h) EDS line scan profile as indicated in (a).

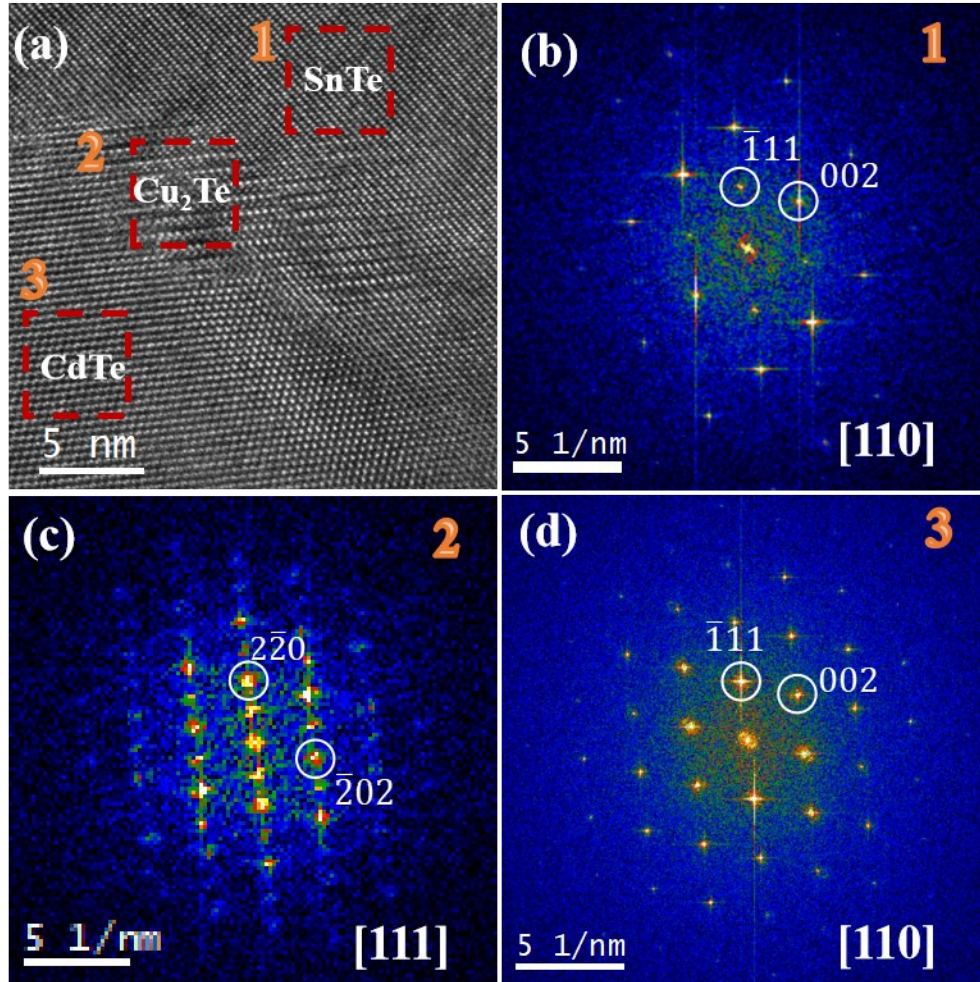


Fig. S6. (a) HRTEM image of the sandwiched structure; (b-d) the corresponding FFT patterns of square regions marked with sequence number 1, 2, 3 in (a), respectively.

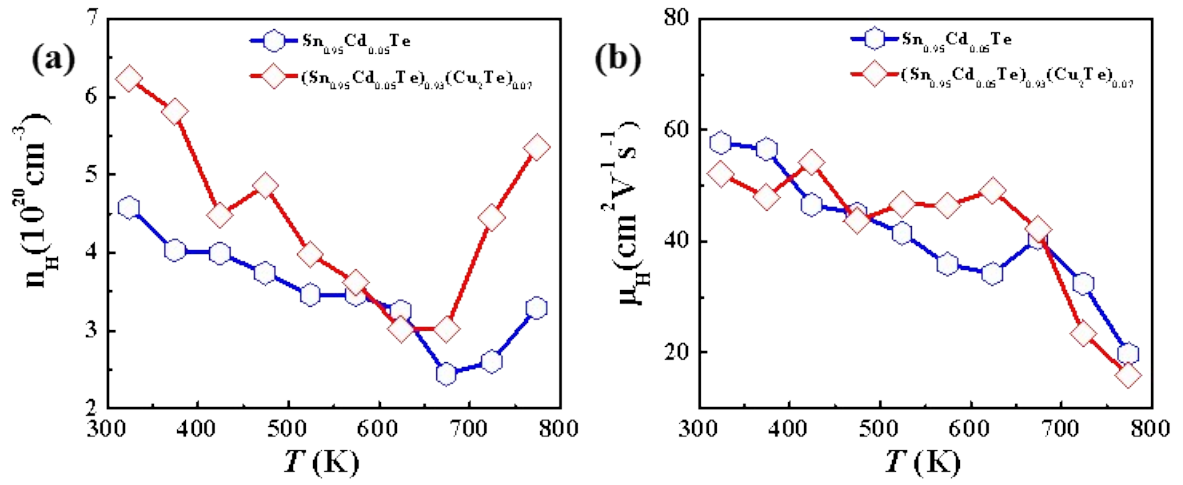


Fig.S7. (a) Temperature-dependent carrier concentration; (b) Temperature-dependent hall mobility for $\text{Sn}_{0.95}\text{Cd}_{0.05}\text{Te}$ and $(\text{Sn}_{0.95}\text{Cd}_{0.05}\text{Te})_{0.93}(\text{Cu}_2\text{Te})_{0.07}$ samples.

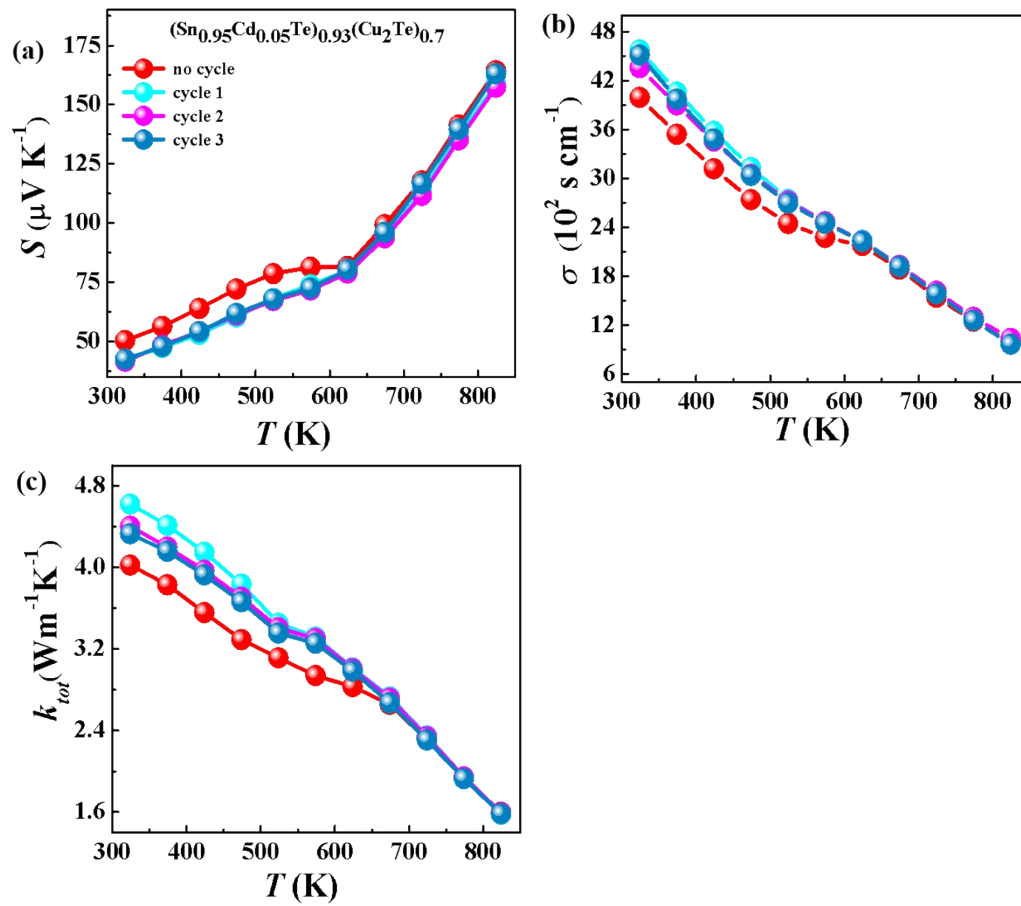


Fig. S8. Cycling stability for $(\text{Sn}_{0.95}\text{Cd}_{0.05}\text{Te})_{0.93}(\text{Cu}_2\text{Te})_{0.07}$ sample. (a) Seebeck coefficient S ; (b) electrical conductivity σ , (c) total thermal conductivity k_{tot} .

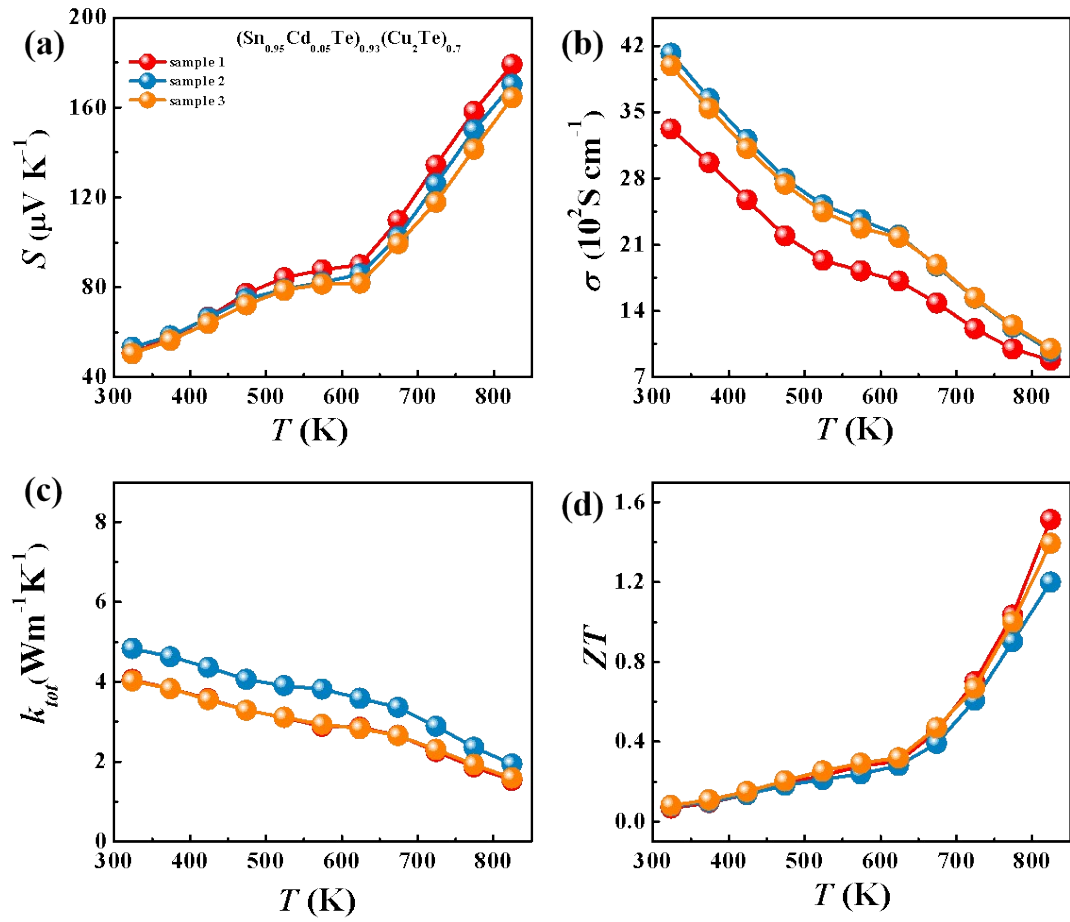


Fig. S9. Repeatability test for $(\text{Sn}_{0.95}\text{Cd}_{0.05}\text{Te})_{0.93}(\text{Cu}_2\text{Te})_{0.07}$ sample. (a) Seebeck coefficient S ; (b) electrical conductivity σ , (c) total thermal conductivity k_{tot} ; (d) ZT . Note that the lowest ZT was used in the main text.

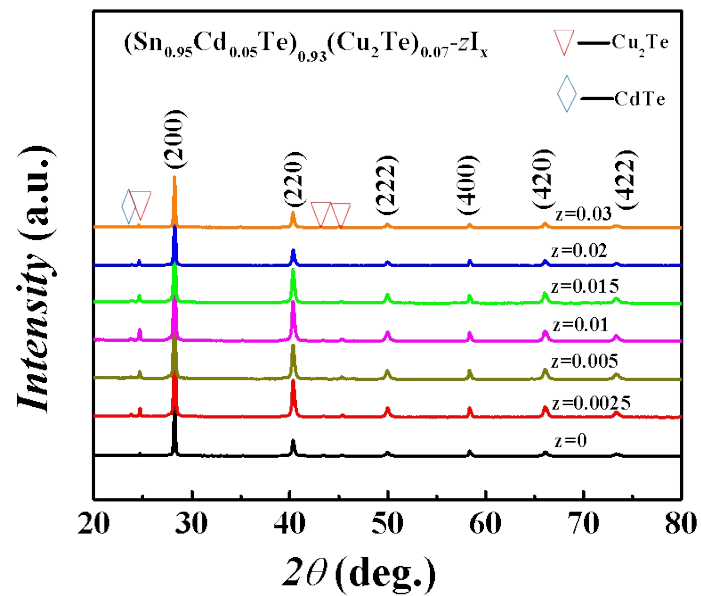


Fig. S10. XRD pattern for $(\text{Sn}_{0.95}\text{Cd}_{0.05}\text{Te})_{0.93}(\text{Cu}_2\text{Te})_{0.07-z}\text{I}_x$ ($z=0, 0.0025, 0.005, 0.01, 0.015, 0.02$ and 0.03) samples.

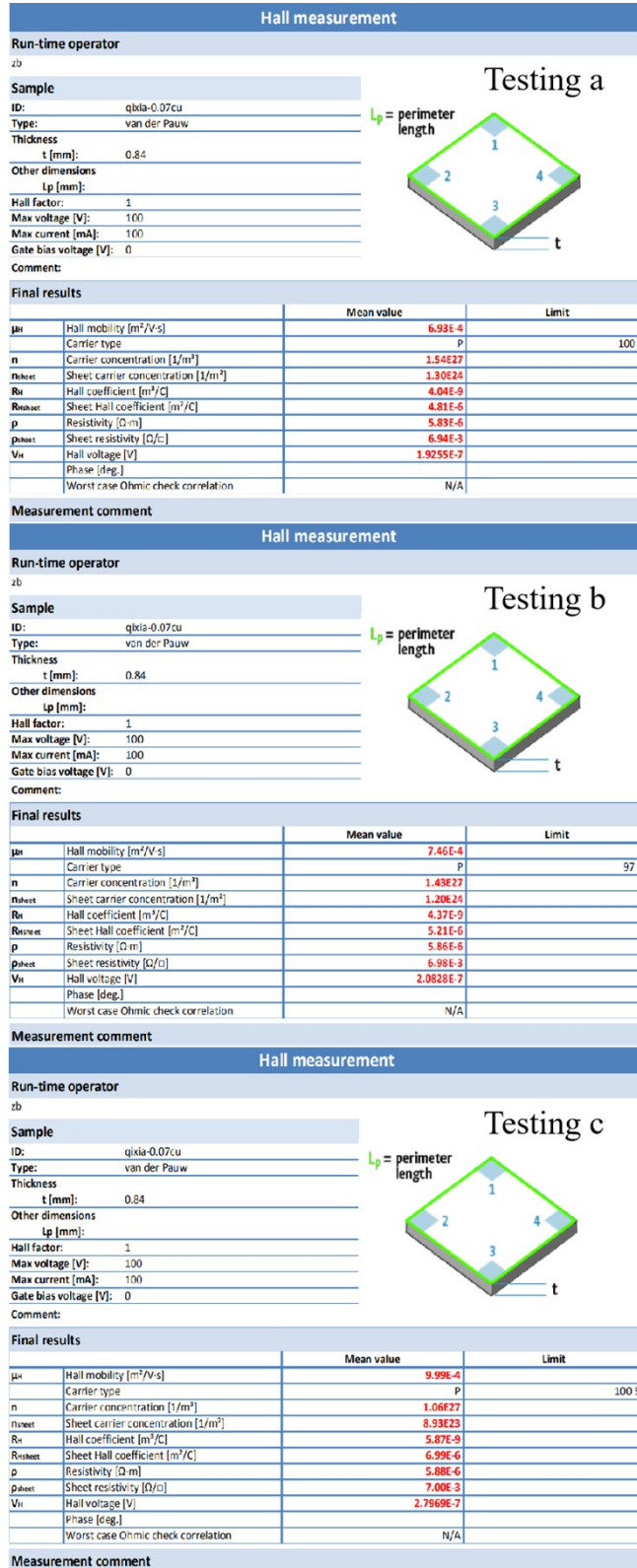


Fig. S11. Original Hall measurement data for $(\text{Sn}_{0.95}\text{Cd}_{0.05}\text{Te})_{0.93}(\text{Cu}_2\text{Te})_{0.07}$ sample of 3 independent tests.

- [1] S. N. Girard, J. Q. He, X. Y. Zhou, D. Shoemaker, C. M. Jaworski, C. Uher, V. P. Dravid, J. P. Heremans and M. G. Kanatzidis. *J Am Chem Soc*, 2011, **133**, 16588-16597.
- [2] H. S. Kim, W. S. Liu, G. Chen, C. W. Chu and Z. F. Ren. *Proc Natl Acad Sci U S A*, 2015, **112**, 8205-8210.